

# LOCALIZED PRECIPITATION, LAKE-EFFECT STORMS, AND EROSION ON MARS.

**Edwin. S. Kite\***, *Earth and Planetary Science, University of California, Berkeley, California, USA* (kite@berkeley.edu), **Scot C.R. Raffkin, Timothy I. Michaels**, *Department of Space Studies, Southwest Research Institute, Boulder, Colorado, USA*, **Michael Manga**, *Earth and Planetary Science, University of California, Berkeley, California, USA.* (\*Abstract author)

**Introduction:** We are modeling localized precipitation on Mars. The hypothesis is that localized water vapor release to the atmosphere in a background climate no warmer than today can result in localized erosion. This requires water vapor supply from an environment not in equilibrium with surface conditions, and because of strong evaporative cooling, water vapor release events would be limited in space or time and usually both. Though previously proposed [e.g. *Gulick and Baker, 1986*], this hypothesis has never been modeled. We report numerical tests of localized precipitation using MRAMS to simulate channel formation downwind of a groundwater outflow site, Juventae Chasma [Milliken *et al.*, 2008].

Martian geology records evidence for numerous short-lived vapor sources [e.g., *Harrison & Grimm, 2008*]. These may be transient, such as an impact lake, or long-lived, such as the base of a wet-based ice-sheet. They can be high-temperature, such as fumaroles (or a lava flow advancing over frozen ground), or involve only moderate temperatures, such as groundwater discharge. We are initially considering only cool ephemeral lakes.

For a given vapor injection rate or lake surface temperature, localized precipitation is more likely on Mars than on Earth. On Earth, localized precipitation involves deep moist convection that usually requires sea surface temperatures  $>299\text{K}$  [Emanuel, 1994]. Cold, thin atmospheres such as that of contemporary Mars are very favorable for deep moist convection in response to disequilibrium water vapor release: low temperature favors crystallization, and low volumetric heat capacity produces greater buoyancy for a given amount of crystallization (Figure 1).

So far we have tested localized precipitation above cold (0-5°C), ephemeral lakes on Mars [Kite *et al*, submitted manuscripts]. As a consequence of the low pressure of the contemporary Mars atmosphere, idealized simulations show that the height and updraft velocities of the resulting storms are comparable to the most intense thunderstorms known on Earth. Our long-term motivation is to better understand Early Mars, but we are using relatively young sites (such as Late Hesperian/Amazonian Juventae Chasma) for geological tests. Here, inputs of water and energy are relatively well constrained. A goal of ongoing work is to understand localized precipitation and erosion in the aftermath of impacts, and we are using well-preserved alluvial fans at Late Amazonian Mojave Crater [McEwen *et al.*, 2007] as a calibration point.

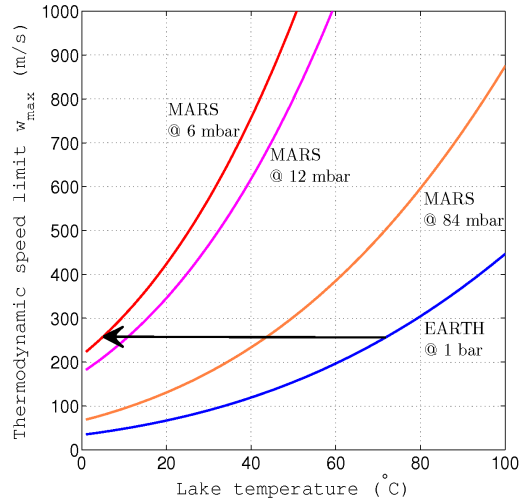


**Figure 1:** To show dependence of lake-driven convection on lake temperature and atmospheric pressure: ordinate shows the thermodynamic speed limit on updraft velocity ( $\sim \sqrt{2\text{CAPE}}$ , where CAPE is Convective Available Potential Energy). Assumptions: Level of Free Convection (LFC) at 0km, Equilibrium Level (EL) at 1.5km, isobaric condensation and precipitation of ascending parcel initially at 50% humidity. The red curve is for today's Mars, the blue curve is for today's Earth, and the magenta curve is the pressure used in our Mars simulations. The black arrow shows that convection above a 5C lake on Mars may be as vigorous as above a 72C lake on Earth. The orange curve corresponds to the threshold pressure above which we suspect localized precipitation on Mars does not occur.

Our modeling supports localized precipitation as an explanation for some Martian erosion, but this mechanism cannot explain all fluvial erosion on Early Mars. A minority of Late Noachian/Early Hesperian valley networks are integrated over thousands of kilometers [e.g., *Barnhart et al, 2009*], suggesting more widespread precipitation during this time window.

## Localized precipitation mechanism:

We hypothesize that precipitation occurs close to vapor sources in Mars-like (cold, low-density) atmospheres:

- 1) Water is released to the surface from an environment not in equilibrium with surface conditions.
- 2) Due to cold background atmospheric temperatures, crystallization of released vapor begins at low altitude.
- 3) Because of low volumetric heat capacity, a strong buoyant plume forms in response to crystalliza-

tion (Figure 1).

4) The buoyant plume drives low-level convergence, so that almost all vapor is fed into the plume.

5) The plume reaches heights at which almost all vapor crystallizes, and the vapor condenses to form large crystals that sink rapidly and precipitate out close to the vapor release point.

These steps are developed quantitatively in [Kite *et al.* 2010a].

**Model:** To test this hypothesis, we use the Mars Regional Atmospheric Modeling System (MRAMS) [Rafkin *et al.*, 2001]. MRAMS explicitly resolves the size spectrum of dust and water ice aerosol for both cloud microphysics and radiative transfer, so it is well-suited for our cloud-forming numerical experiments [Michaels and Rafkin, 2008]. Boundary conditions are from the NASA Ames MGCM.

Pressure is doubled from today's values to allow stable surface liquid water. We do not include water vapor in the mass or momentum equations (so virtual temperature and pressure effects are not considered),

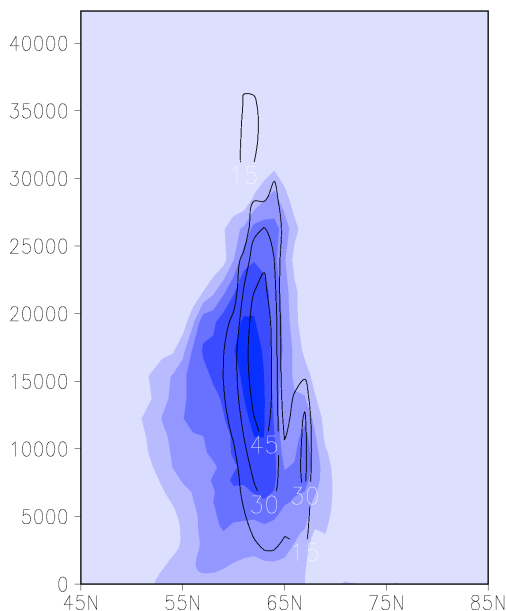


**Figure 2.** N-S cross section through lake storm (idealized boundary conditions). Blue tint corresponds to increasing water ice fraction (interval 0.002, maximum value 0.011). Labeled contours correspond to bulk vertical velocity in m/s. y-axis is vertical distance in m. x-axis is horizontal distance in simulation units: 10 simulation units = 59 km. Lake extends from 69N to 79N on this scale.

which probably leads to an underestimate of the evaporation rate. Lake surface temperature is fixed in our simulations, which is an adequate approximation if (a) the lake is deep and well-mixed or (b) the lake surface is constantly refreshed by discharge of warm, perhaps gas-charged water from an aquifer.

**Results of idealized simulations of lake storms on Mars:** For our reference simulation, we introduce a square lake with sides 65km into a flat landscape

with Mars-average surface properties. The resulting buoyant plume (Figure 2) lifts vapor above condensation level, forming a 20km-high optically-thick cloud. Ice grains grow to 200  $\mu\text{m}$  radius and fall typically <100 km from the lake at mean rates up to 1.5 mm/hr water equivalent (maximum rates up to 6 mm/hr water equivalent). Most of the released vapor is trapped locally as snow, so is unavailable to drive global climate change. These results are qualitatively insensitive to geophysically reasonable changes in lake latitude, lake surface roughness parameterization, solar luminosity, season, model horizontal resolution, model vertical resolution, lake geometry (line versus square), and lake surface temperature. For square lakes of size  $10^{2.5} - 10^{3.5} \text{ km}^2$  plume vertical velocity scales linearly with lake area. However, convection does not reach above the planetary boundary layer for lakes  $\ll 10^3 \text{ km}^2$  or for atmospheric pressure  $> O(10^2)$  mbar. Instead, in these cases, vapor is advected downwind with little cloud formation.

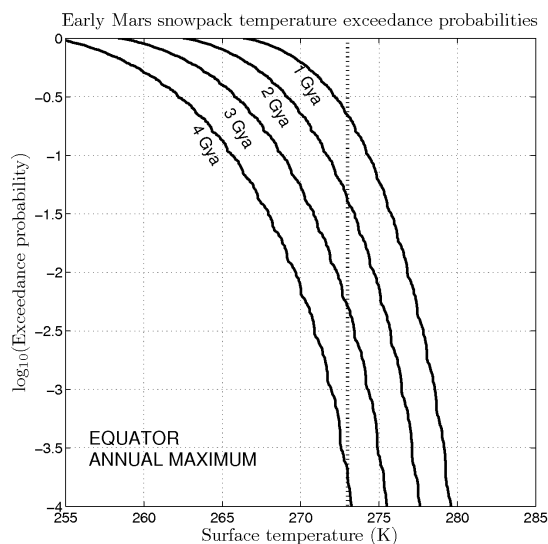


**Figure 3.** Exceedance probabilities for annual peak temperature of snowpack at Mars' equator. A dust-like albedo (0.28) is assumed. Vertical dashed line corresponds to the melting point. For progressively earlier times (reduced solar luminosity), the probability of melting decreases.

**Snowpack temperature exceedance probabilities:** Precipitation in our model falls as snow. However, the geologic record demands surface runoff. Melting is straightforward if the snow falls onto the ejecta of a just-formed impact crater, but it is less obvious if melting will occur if the vapor is released during a groundwater outflow event.

To determine the probability of melting in this case, we run a 1D ground temperature model for all orbital conditions, seasons, and past solar luminosities, assuming vapor release near the equator. We assume that localized snowpack persists for at least 1 year after the vapor release event. We multiply the

calculated maximum annual temperatures with published orbital parameter probability distributions [Laskar *et al.*, 2004]. The resulting melting probability (for dirty snowpack albedo 0.28, still conditions, and a 6 mbar CO<sub>2</sub> atmosphere) is shown in Figure 3. Evaporative cooling prevents melting for all but the most favorable orbital conditions. Higher pressures would suppress evaporative cooling, allowing melting over a wider range of orbital conditions [Hecht, 2002]. Because localized precipitation can occur at any latitude, melting probability is higher for localized precipitation than for cold-trapped snow that migrates in response to orbital forcing.

**Valles Marineris snowstorms:** We test localized precipitation at Juventae (northern Valles Marineris). Here, a 5km-deep chasm drains across a spillway to form an outflow channel, which is strong evidence for the past evidence of a lake within the chasm [Harrison & Grimm, 2008]. Channel networks on the plateau adjacent to the Juventae chasm have the highest drainage densities reported on Mars [Malin *et al.*, 2010]. They are embedded within opaline layered deposits, which are among the youngest aqueous minerals reported from Mars [Milliken *et al.*, 2008]. We hypothesize that the plateau channels formed as a result of localized lake-effect storms. In our best-fitting simulation, we flood Juventae Chasma to the depth of the observed spillway. At Juventae Chasma, mean snowfall reaches a maximum of 0.9mm/hr water equivalent on the SW rim of the chasm. Radiative effects of the thick cloud cover raise maximum (minimum, mean) plateau surface temperatures by up to 24K (9K, 17K) locally. The key result (Figure 4) is that the area of maximum modeled precipitation shows a striking correspondence to the mapped Juventae plateau channel networks. The interaction of lake-driven convergence, topography and the regional wind field sweeps released vapor into a narrow plume and leads to maximum on-land precipitation at the observed channel networks (Figure 4). Three independent methods (Monte Carlo; the metric of [Pielke & Mahrer, 1978]; and comparison of data and model azimuths) show this fit is unlikely to be due to chance. We have carried out an additional test to Echus Chasma, and preliminary results also show a good correspondence between predicted precipitation locations and observed channels. More details of these tests are given in [Kite *et al.* 2010b].

**Ongoing work - Extension to impact-induced precipitation:** Noachian and Early Hesperian craters on Mars have deeply dissected rims and infilled floors which are usually attributed to global erosion. We seek to understand if these craters could have partially self-erased through localized, impact-induced processes [Senft and Stewart, 2008]. This is ongoing work,

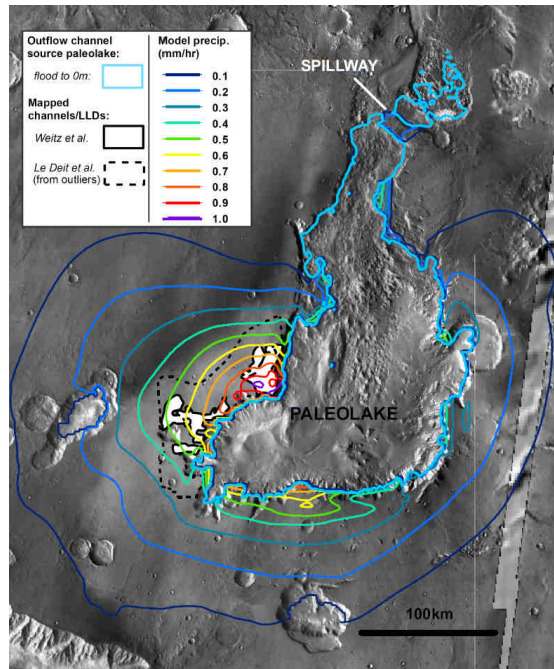


**Figure 4.** Modeled precipitation contours overlain on observed geology at Juventae (4S, 60W). White shading with thick solid black outline corresponds to area of layered deposits and inverted channels. The dashed black line corresponds to the pre-erosion area of layered deposits inferred from outlier buttes and pedestal craters. The thick cyan line denotes the flooded area for this simulation (the -1000m contour). The colored lines are modeled time-averaged precipitation contours at intervals of 0.1 mm/hr water equivalent. Precipitation falling back into the lake is not shown. The spatial maximum in mean precipitation is ~1.0 mm/hr.

and our current focus is to use ~2-3 Mya Mojave Crater (date courtesy of Stephanie C. Werner) as a relatively young and well-preserved calibration point. Mojave's inner rim is heavily modified by dendritic channels and alluvial fans, but we have found only sparse or questionable evidence of recent fluvial modification in the region surrounding the crater (Figure 5). This is prima facie geological evidence for localized precipitation. We use Mojave-specific impact hydrocode simulations (CTH) to set the ground temperature boundary condition (tailored simulations courtesy of Sarah Stewart, Harvard). MRAMS simulations using an ephemeral lake vapor injection boundary condition show maximum water-equivalent precipitation rates ~1mm/hr. Going further will require a model linking snowfall rates, ejecta temperature and erosion, and accounting for direct rainout of water condensing from the impact plume.

It is conceivable that Hesperian fluvial activity at Eberswalde is related to the nearby (Hesperian) Holden impact. If the MSL spacecraft is directed to Holden or Eberswalde, we plan to test this conjecture.

**Acknowledgements.** We acknowledge significant contributions from Sarah Stewart (Harvard), Stephanie Werner (Oslo), Susan Conway (Nantes), and Bill Dietrich (UC Berkeley).

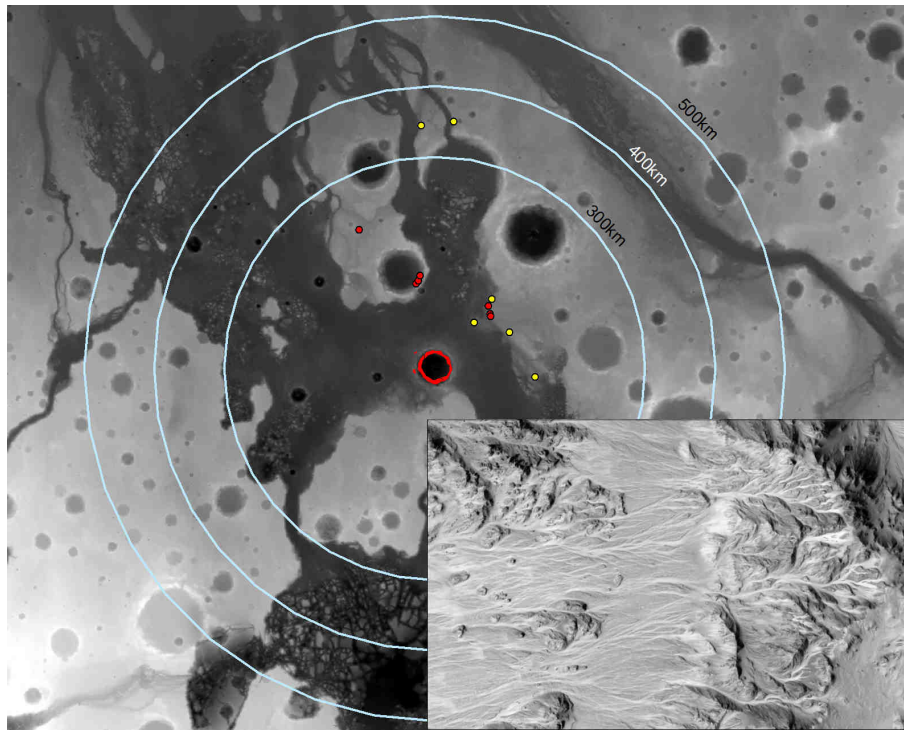


**Figure 5:** Mojave Crater (central 60km-diameter crater; 7.5N, 33W) in regional context, showing rapid falloff of young fluvial activity (red) with distance (pale blue rings) from the inner crater wall (red ring). Probable young fluvial activity shown by red dots, possible by yellow dots. Background is MOLA topography (white is 0m elevation, black is -5000m elevation). In virtue of this isolation and the young age of the system (~3 Mya: S.C. Werner, via email), fluvial activity within Mojave appears to have been triggered by the Mojave impact. Both 1D and 3D numerical models are being used to test this hypothesis. Inset image, subset of HiRISE image PSP\_001415\_1875 shows detail of fluvial activity.

**References:** Barnhart, C.J., A.D. Howard & J.M. Moore (2009), Long-term precipitation and late-stage valley network formation: Landform simulations of Parana Basin, Mars, *J. Geophys. Res.* 114, E01003, doi:10.1029/2008JE003122.

Emanuel, K.A. (1994), *Atmospheric convection*, Oxford University Press.

Harrison, K.P., & M.G. Chapman (2008), Evidence for ponding and catastrophic floods in central Valles Marineris, Mars, *Icarus* 198, 351-364.

Hecht, M.H. (2002), Metastability of liquid water on Mars, *Icarus* 156, 373-386.

Kite, E.S., et al., in review, Localized precipitation and runoff on Mars, available on arXiv astro-ph:EP (<http://arxiv.org/abs/1012.5077>)

Kite, E.S., et al., in review, Chaos, storms and climate on Mars, available on arXiv astro-ph:EP (<http://arxiv.org/abs/1101.0253>)

Gulick, V.C., and V.R. Baker (1986), Fluvial valleys and Martian paleoclimates, *Nature* 341, 514-516.

Laskar, J. et al. (2004), Long term evolution and chaotic diffusion of the insolation quantities of Mars, *Icarus* 170, 343-364.

McEwen, A.S. et al. (2007), A Closer Look at Water-Related Geologic Activity on Mars, *Science* 317, 1706-1709.

Malin, M.C., et al. (2010), An overview of the 1985-2006 Mars Orbiter Camera science investigation, *Mars* 5, 1-60, doi:10.1555/mars.2010.0001

Michaels, T.I., & S.C.R. Rafkin (2008), MRAMS today - One example of current Mars mesoscale modeling capabilities, *Third International Workshop on Mars Atmosphere: Modeling and Observations*, Williamsburg, Virginia, 9116.

Milliken, R.E., et al. (2008), Opaline silica in young deposits on Mars, *Geology* 36, 847-850.

Pielke, R.A. & Y. Mahrer (1978), Verification analysis of University-of-Virginia 3-dimensional mesoscale model prediction over South Florida for 1 July 1973, *Monthly Weather Rev.* 106, 1568-1589.

Rafkin, S. C. R., Haberle, R. M., and T. I. Michaels (2001), The Mars Regional Atmospheric Modeling System (MRAMS): Model description and selected simulations, *1088 Icarus*, 151, 228-256.

Senft, L., & S. Stewart (2008), Impact Crater Formation in Icy Layered Terrains on Mars, *Meteoritics and Planetary Science*, 43 (12), 1993-2013.